Active output LLC converter topology

Hannes Börngen, Eyke Liegmann, Sriram Jagannath, Ralph Kennel

Chair of High-Power Converter Systems , Technical University of Munich
Arcisstr. 21, 80333 Munich, Germany

Email: hannes.boerngen@tum.de

Keywords

≪DC-DC converter≫, ≪Resonant converter≫, ≪ZVS converters≫, ≪Soft switching≫.

Abstract

This paper presents an "active output" LLC topology, i.e. a variant of the load-resonant LLC converter with *asynchronous* rectification stage. In this topology, the output switches actively block and thus change the apparent parameters of the resonant tank. Advantages, such as an increased design space for converter optimisation, are gained.

Introduction

The state-of-the-art LLC converter, Fig. 1, is a dc-dc converter belonging to a group of so called load-resonant converters. Advantages of the LLC topology are the low component count, mainly a resonant tank comprising two inductances, L_s and L_p, and one capacitance, C_s, and the fact that the topology and its modes of operation lend themselves to soft switching. For majority charge carrier devices, zero-voltage switching (ZVS) transitions for the primary-side switches (S_1–S_4) are most beneficial to achieve. On the output side, diodes or switches emulating diode behaviour ($S_{o,1}$, $S_{o,2}$) are used to rectify the transformer's secondary-side current. The secondary-side switches usually achieve soft switching when switching from *off* to *on* state. These characteristics prime the LLC topology as a compact and high efficiency solution for a broad range of applications.

To mitigate a major issue of the LLC, namely the influence of the ratio of the resonant inductances on the achievable voltage transfer ratio *and* efficiency, a novel topology and control approach will be presented. The contribution can be summarised as making the resonant tank's behaviour controllable via adding reverse blocking switches on the output side and in this way realising an active output.

In literature, different means can be found that achieve an adaptive damping-factor, namely secondary-side phase-shift modulation (SSPSM) [1], secondary-side pulse width modulation (SSPWM) [2], and

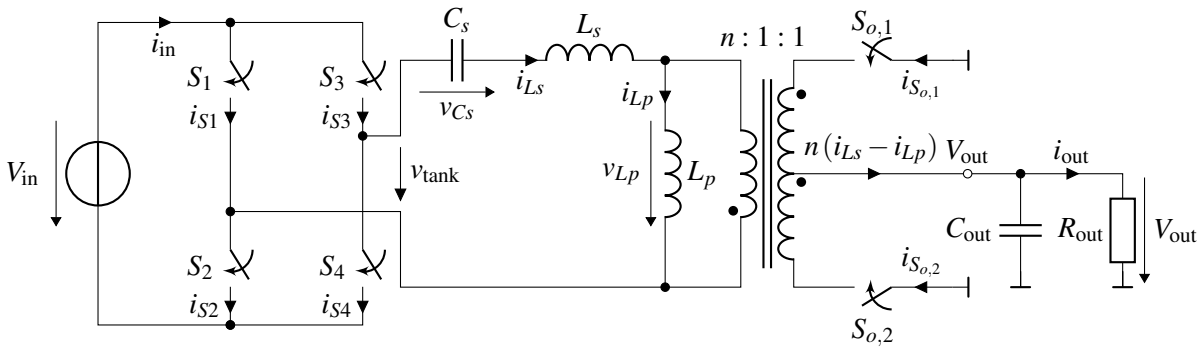

Fig. 1: State-of-the-art LLC converter topology.

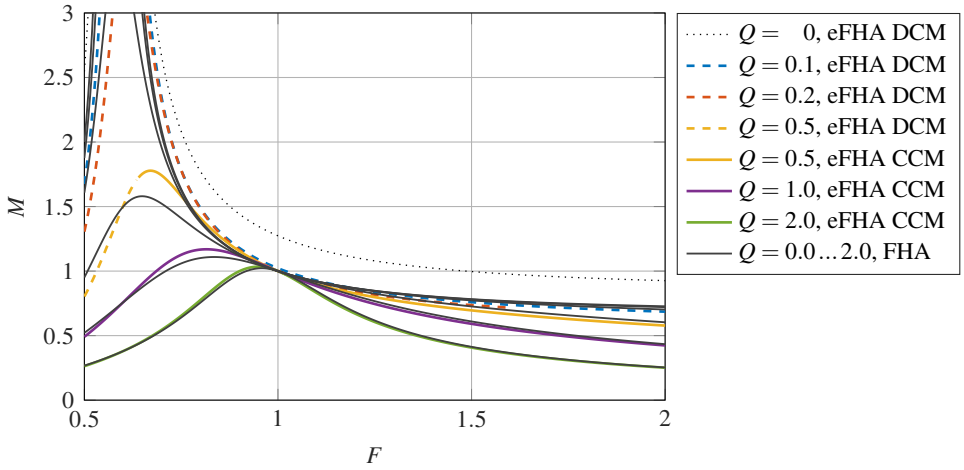

Fig. 2: Voltage transfer ratio of the frequency-modulated LLC; FHA, coded via solid black lines —, eFHA, coded via *coloured* lines, where discontinuous conduction mode (DCM) is coded via dashed lines, e.g. - - -, and continuous conduction mode (CCM) is coded via solid lines, e.g. —.

a whole family of secondary-side "active boost rectifier" topologies [3]. In the case of SSPSM, the advantage of having voltage regulation without a change in switching frequency of the primary-side switches is employed to increase the hold up time for a fixed frequency LLC converter. For SSPWM, an adaptive voltage doubler topology on the output side is implemented for a fixed frequency LLC and is controlled to achieve the voltage regulation of the output side.

State-of-the-art LLC modulation techniques

In the following, two state-of-the-art modulation schemes for the LLC converter will be presented: frequency modulation and phase-shift modulation.

Frequency modulation

One major drawback of the LLC topology is the limited range of the output to input voltage ratio, which is linked to the fact that the flow of power is usually controlled via frequency modulation (fm). The voltage transfer function, $V_{\text{out}}/V_{\text{in}}$, of the frequency-modulated LLC can, by means of a first harmonic approximation (FHA) [4], be calculated as

$$M_{\text{LLC,fm}} = \frac{1}{n\sqrt{\left[1+\kappa\left(1-\frac{1}{F^2}\right)\right]^2+\frac{\pi^4 Q^2}{64}\left(F-\frac{1}{F}\right)^2}} \tag{1}$$

with κ equalling the ratio of the resonant inductances, L_s/L_p, n being the transformer's transfer ratio, and with the control parameter F, the normalised switching frequency. The normalised switching frequency is defined as $f_{\text{sw}}/f_{s,0}$, where $f_{s,0}$ is the series resonance frequency $1/2\pi\sqrt{L_s C_s}$ and f_{sw} is the reciprocal of the duration of the switching period, T_{sw}. The quality factor Q of the resonant circuit is defined as $Z_0 P_{\text{out}}/n^2 V_{\text{out}}^2$, where Z_0 is $\sqrt{L_s/C_s}$. Thus, Q is also a measure of the transferred power.

The voltage transfer ratio of the frequency-modulated LLC is shown in Fig. 2, with Q as a parameter. In the plot, two different means of calculating the transfer ratio are employed, the aforementioned FHA and the extended FHA (eFHA) [5]. When switching with frequencies higher than F equal to 1 (*load independent point*), the resonant tank always exhibits inductive behaviour, which is necessary to achieve ZVS of the input switches. Below the *load independent point*, the resonant tank can show inductive behaviour as well, if the operating point is on the right-hand side of the maximum of the respective curve. For a fixed voltage transfer ratio, a reduction in transferred power is achieved with higher switching frequencies and is bounded by a lower limit, which depends on the ratio L_s/L_p and is as such fixed in the design stage. This behaviour can be visualised by the no-load curve, i.e. Q is 0, ·····, where the voltage transfer ratio tends towards a non-zero value for higher switching frequencies. Changing the inductance

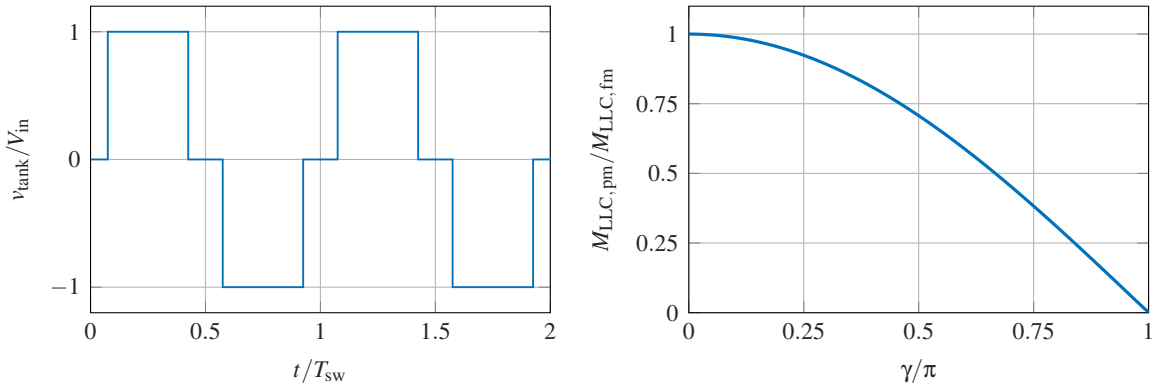

(a) Voltage applied to resonant tank, $\gamma = 0.3\,\pi$.

(b) Voltage transfer ratio.

Fig. 3: Phase-shift modulation of the LLC.

ratio in order to increase the range of achievable voltage ratios, e.g. by decreasing the value of L_p, is detrimental to the efficiency of the converter. How this constraint can be taken into account for the design of an LLC has been covered in [6].

Primary-side phase-shift modulation

In recent years, different methods have been investigated to mitigate this disadvantageous characteristic of the frequency-modulated LLC. One approach is to employ a different modulation technique, namely a phase-shift modulation (pm) for the primary-side switches [7], [8]. By this, the voltage applied to the terminals of the resonant tank can be clamped to 0 V in addition to positive and negative voltages. The voltage applied to the resonant tank depends on the phase-shift, γ, and is:

$$v_{\text{tank}}(t) = \begin{cases} 0 & 0 & < & t \bmod T_{\text{sw}} & \leq \frac{T_{\text{sw}}}{2}\frac{\gamma}{2\pi} \\ V_{\text{in}} & \frac{T_{\text{sw}}}{2}\frac{\gamma}{2\pi} & < & t \bmod T_{\text{sw}} & \leq \frac{T_{\text{sw}}}{2}\left(1-\frac{\gamma}{2\pi}\right) \\ 0 & \frac{T_{\text{sw}}}{2}\left(1-\frac{\gamma}{2\pi}\right) & < & t \bmod T_{\text{sw}} & \leq \frac{T_{\text{sw}}}{2}\left(1+\frac{\gamma}{2\pi}\right) \\ -V_{\text{in}} & \frac{T_{\text{sw}}}{2}\left(1+\frac{\gamma}{2\pi}\right) & < & t \bmod T_{\text{sw}} & \leq \frac{T_{\text{sw}}}{2}\left(2-\frac{\gamma}{2\pi}\right) \\ 0 & \frac{T_{\text{sw}}}{2}\left(2-\frac{\gamma}{2\pi}\right) & < & t \bmod T_{\text{sw}} & \leq T_{\text{sw}}. \end{cases} \tag{2}$$

An exemplary tank voltage is drawn in Fig. 3a. When using a similar approach to the FHA we can yield an analytical formula for the phase-shift modulated LLC converter. I.e. the time-domain voltage leads to a voltage gain $M_{\text{LLC,ph}}$ that exhibits the same behaviour as the frequency-modulated LLC, $M_{\text{LLC,fm}}$, with an additional multiplicative term as:

$$M_{\text{LLC,pm}} = \frac{\sqrt{2}}{2}\sqrt{\cos\gamma + 1}\, M_{\text{LLC,fm}}, \tag{3}$$

which is shown in Fig. 3b. It is apparent that the drawback of a design-determined lower output voltage is fixed, as the control input γ allows achieving output voltages down to 0 V.

Some literature can be found on the phase-shift LLC [7], [8], but to the knowledge of the authors, no in-depth investigation has been published that discloses a design optimisation strategy. The major disadvantage when designing the phase-shifted LLC is that a considerable phase-shift must be used for nominal input voltage, since the minimum input voltage should be covered by operation with zero phase-shift. As with the phase-shifted full-bridge converter, an asymmetry exists with regard to ZVS [9], the so called "active-to-passive", *strong*, and "passive-to-active", *weak*, transition of the input full bridge. This leads to a constrained design space in which κ has to be chosen large for ZVS, which in turn leads to low efficiency caused by an increase in circulating currents. To mitigate this issue, a topology and modulation scheme will be presented in the following section.

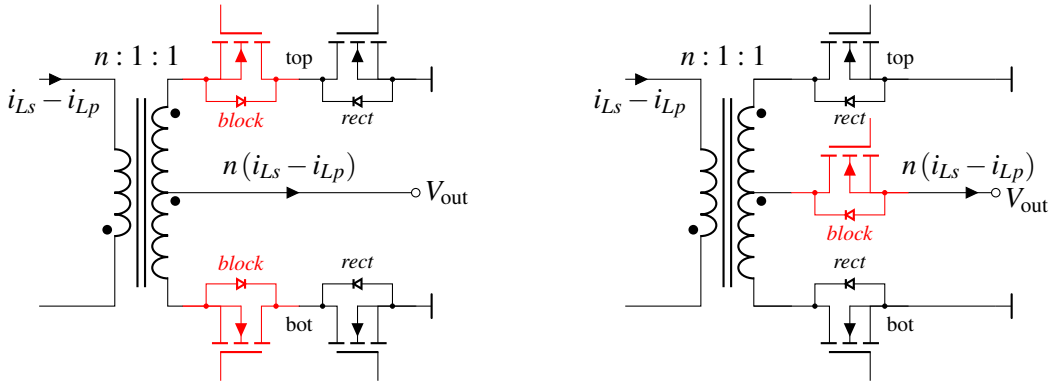

(a) Proposed active output configuration.

(b) Active output alternative configuration.

Fig. 4: Output configurations of an active output LLC converter; proposed changes in red.

Proposed active output LLC converter

The main advantage of the proposed solution comes into play if a wide voltage transfer range is required, as a boosting of the output voltage can be achieved at low switching frequencies, as well as a step-down at higher switching frequencies. Another benefit lies in the fact that the resonant tank can be forced to consist of C_s, L_s, *and* L_p instead of solely C_s and L_s. The additional energy stored in the resonant tank enables a wider design range where ZVS of the primary-side switches can be achieved. Through this, the problems arising from the *weak leg* of the phase-shift modulation can largely be avoided, including the rather constrained suitable range of κ.

Topology and blocking switch implementation

State-of-the-art LLC converters use a *synchronous rectification*, i.e. an active switch that emulates diode behaviour. For the implementation of this, it comes in handy that most switches possess an anti-parallel diode and conduct current in the reverse direction when turned on. Both rectification schemes, using diodes and synchronous rectification, are in the following referred to as *passive rectification*.

In order to be able to actively block the output current path, normal, reverse conducting power switches cannot be used. Two approaches can be taken here; the development of reverse blocking switches or adding anti-series connected reverse conducting switches. One possible configuration of the proposed active output topology is presented in Fig. 4a, where the combination of switches act as a reverse blocking switch. This reverse blocking is activated as long as the gate signal of the respective blocking switch (*block*) is low. If the gate signal of the blocking switch is high, the respective rectifying switch (*rect*) can be used as a synchronous rectifier. It is possible to reconfigure the output in a manner that only *one* blocking switch is sufficient, as shown in Fig. 4b. This would entail the additional advantage that the *blocking* switch gate signal can be referenced to a constant voltage, namely V_{out}. The drawback of the latter solution is a more complicated timing of the gate drive pattern.

In Fig. 5, the active output LLC with the proposed blocking output configuration is shown in its entirety. The voltages across the blocking switches, v_{block}, have been defined as they would be generally defined for active switches, such as MOSFETs. In contrast, the voltages across the rectifying switches, v_{rect}, have been defined as more akin to the case where diodes are used.

Timing definitions

The gate signals of the blocking switch or, more precisely, the extensions of the blocking time are the control input for the active output LLC's secondary side, alongside with the switching frequency and the phase-shift modulation of the input full bridge. To illustrate the behaviour of the proposed topology, key voltage and current waveforms of an active output LLC are shown in Fig. 6. Additionally, the gate signals of the blocking switches are plotted.

In the diagrammed operating point, the active output LLC operates in DCM, where the bottom *rectifying* switch is "naturally" not conducting from ca. $0.245\,T_{\text{sw}}$ to $0.5\,T_{\text{sw}}$. The duration thereof is $T_{\alpha,1} = \alpha_1/2\pi\,T_{\text{sw}}$.

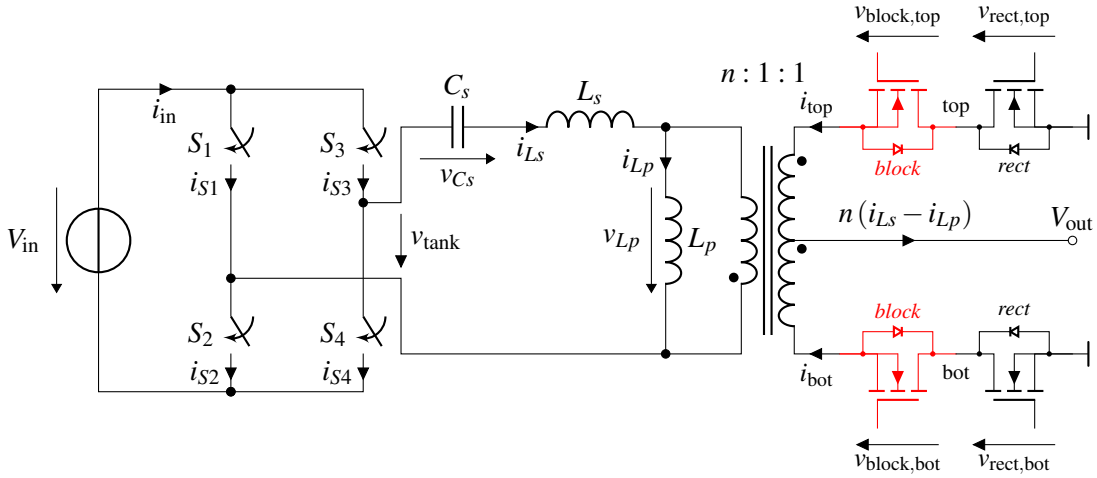

Fig. 5: Active output LLC converter topology; proposed changes in red.

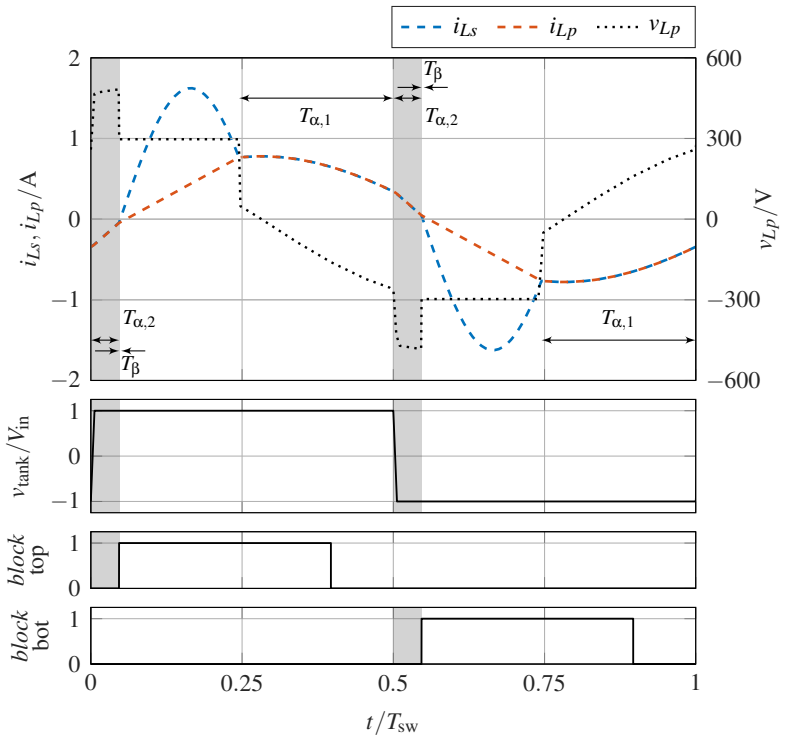

Fig. 6: Resonant tank behaviour and timing definitions of the active output LLC; $\alpha_2 = 0.08\,\pi$, $F = 0.465$, $\kappa = 0.166$, $Q = 0.17$. The output is *naturally* blocking during α_1 and is *actively* blocked during α_2. The currents i_{Ls} and i_{Lp} are equal during α and the energy stored in both inductances aids in achieving ZVS transitions.

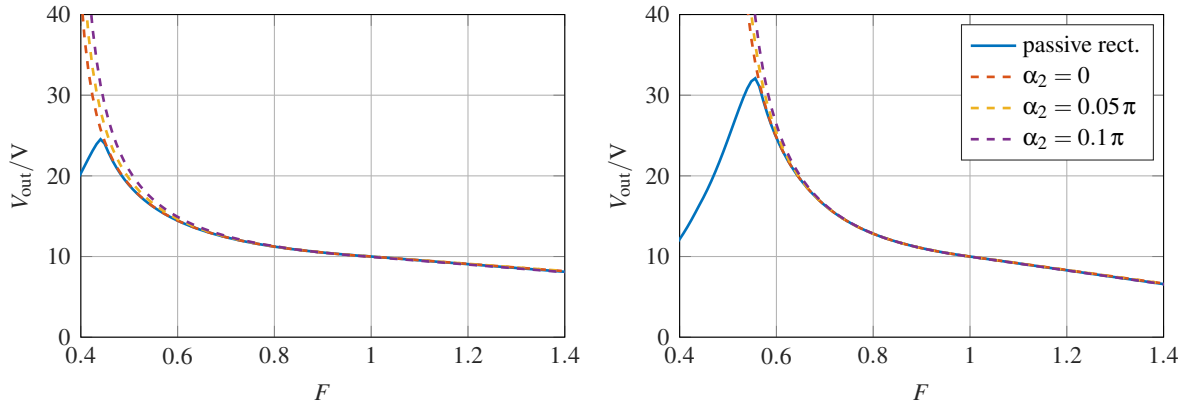

(a) $\kappa = 0.166$. (b) $\kappa = 0.333$.

Fig. 7: Frequency-domain behaviour with improved boost capabilities; $Q = 0.17$, $V_{in} = 120\,V$.

From $0.5\,T_{sw}$ until $0.54\,T_{sw}$ the bottom output switch is blocking and thus forces L_s to be equal to L_p. The time spans during which one of the output switches is actively blocking are shaded in grey. The duration, $T_{\alpha,2} = \alpha_2/2\pi T_{sw}$, is the previously mentioned control input of the active output LLC, where α_2 denotes the delay from the, if applicable, *weak* half bridge transition to the switch *on* of the output blocking switch. While i_{Ls} is equal to i_{Lp}, both L_s and L_p take part in the resonance with C_s. The energy stored in both L_s and L_p supports the charging of the primary-side switch output capacitances C_{oss} and thus helps to achieve a ZVS transition.

As soon as the respective output blocking switch gate signal is *high*, the output current rises and i_{Ls} is not equal to i_{Lp} anymore. In the example in Fig. 6, i_{Ls} drops quickly below 0 A after turning on of the respective output blocking switch, the duration of this time span is T_β.

Frequency-domain investigation

The previous section showed that the actively blocking output changes the waveforms of the resonant tank significantly. The effects in the frequency domain are discussed in the following. To this end, Fig. 7 depicts the output voltages plotted against the switching frequency F for two for different resonant inductance ratios, κ. In Fig. 7a we see the behaviour for a value of κ that is equal to 0.166, in Fig. 7b for a value of κ being equal to 0.333. From both plots it is apparent that for a normalised switching frequency of 1 we are at (or in fact rather close to) the load independent point, and both subplots exhibit the same voltage transfer ratio of $1/n = 1/12$. In addition, it is evident that the influence of the additional blocking time is marginal for the frequency range close to and above the load independent point if no phase-shit is used. The voltage transfer ratio with primary-side phase-shift will be covered in a following section.

It is important to note, that a significant increase of the voltage transfer ratio can be observed at switching frequencies close to the maximum voltage transfer ratio of the respective *passive rectification* curve (—). This characteristic can be used to achieve a higher voltage transfer ratio, without having to increase κ to reach the desired output voltage levels. Comparing the behaviour of the output blocking curves in Fig. 7a with the *passive rectification* curve in Fig. 7b, it is apparent that the same output voltages can be achieved with a κ that is 50 % smaller. This augments the design space of the LLC significantly, as a decrease in κ comes with an increase in efficiency.

Time-domain investigation

In the following, focus is put on the time-domain behaviour of the active output LLC, to understand how the proposed topology influences the resonant tank's waveforms. In the first subsection, the operating mode with switching frequencies below the series resonance is investigated. To achieve higher output voltages, the proposed LLC topology is operated solely with frequency modulation. Subsequently, the behaviour of the topology with additional phase-shift modulation of the input full bridge is scrutinised.

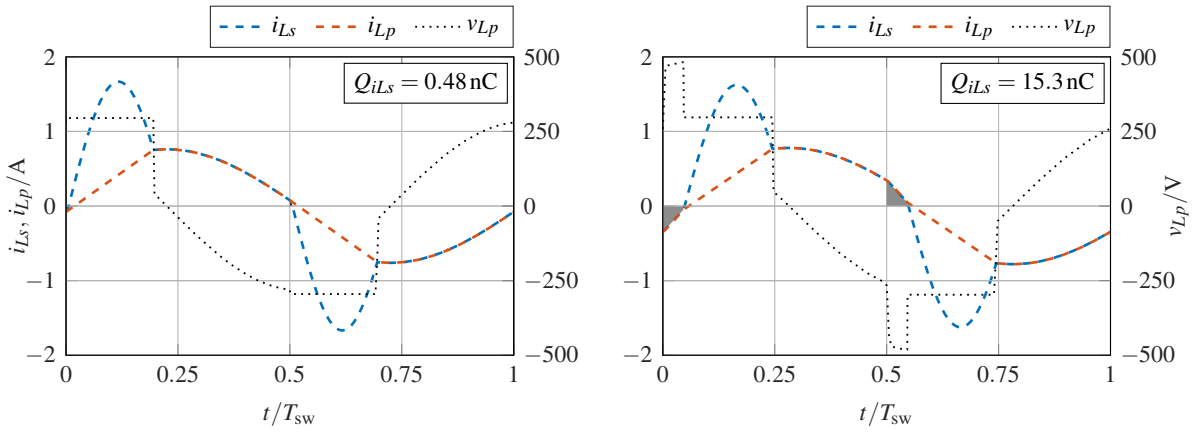

(a) Passive rectification, $F = 0.445$.

(b) $\alpha_2 = 0.08\,\pi$, $F = 0.465$.

Fig. 8: ZVS charge of passive rectification and active output LLC, with a 30-fold increase in case of active rectification; $\kappa = 0.166$, $Q = 0.17$, $V_{\mathrm{in}} = 120\,\mathrm{V}$.

Behaviour below series resonance frequency

For low input voltages, the LLC is operated close to its lower resonance frequency $1/2\pi\sqrt{C_s(L_s+L_p)}$, i.e. close to the maximum voltage transfer ratio. Here, one important characteristic is the increased boost capability to achieve the desired output voltage. Additionally, with the extended blocking time comes an increase in the available energy for the ZVS transition.

This improved ZVS transition is based on two different effects that are caused by the active blocking. Firstly, we delay the tank's current response to the applied voltage, which is directly related to α_2. This can be seen as making the resonant tank more inductive. Secondly, even without the delay of the tank's current with respect to the input voltage, we force i_{Ls} to drop more slowly, by connecting L_s essentially in series with L_p.

To show how pronounced the combination of both effects is, Fig. 8 depicts two operating points for an output voltage of 25 V. In Fig. 8a, the waveforms of the resonant tank's inductive components are drawn for a standard LLC. At t equal to $0.5\,T_{\mathrm{sw}}$, a switching transition of the primary-side full bridge takes place, which can be seen at the small, step like change of v_{Lp}, the voltage across L_p. It is apparent that at this time instance the currents of both, L_s and L_p, have decreased close to 0 A. The charge that flows through L_s until the current has fully dropped to 0 A, i.e. the charge for the ZVS transition, is ca. 0.48 nC. In Fig. 8b, the same waveforms are drawn for the proposed topology. As before, at $0.5\,T_{\mathrm{sw}}$ a switching transition of the primary-side full bridge takes place, which can be seen at the steep change of the voltage across L_p. At this time instance the currents of both, L_s and L_p, are still significantly larger. The charge through L_s is 15.3 nC, visualised by a dark grey area, and is thus a factor of thirty times larger compared to the standard solution and shows how the ZVS behaviour is greatly improved.

Behaviour with primary-side phase-shift

For high input voltages, the LLC is operated *at* or *above* its series resonance frequency and, additionally, with a significant primary-side phase-shift. In the following, only the operation at F equal to 1 will be presented as both regions exhibit similar characteristics.

To make the interaction between the active output LLC's control input α_2 and the primary-side phase-shift γ evident, Fig. 9a is plotted. We see that both an increase in α_2 and γ leads to a step-down of the output voltage. If the output is controlled to 20 V, a primary-side phase-shift of $0.6\,\pi$ (●) will be employed for a standard output. The charge Q_{ZVS} present for the *weak leg* ZVS-transition, Fig. 9b, is 2.2 nC (●) in this operating point. In case of the active output scheme with an α_2 of $0.1\,\pi$, a significantly smaller primary-side phase-shift of $0.5\,\pi$ (▲) is sufficient. At this operating point, Q_{ZVS} is larger with 9.2 nC (▲).

If we assume that a charge of 14 nC (indicated by the black dashed line) is necessary for the ZVS tran-

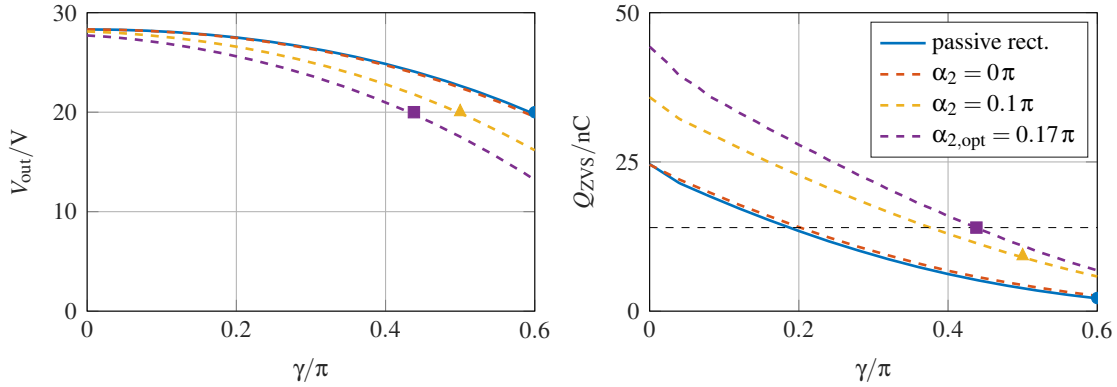

(a) Output voltage.

(b) ZVS charge for the *weak leg*.

Fig. 9: Behaviour with primary-side phase-shift γ, dependency of increase of ZVS charge with parameter α_2; $F = 1$, $\kappa = 0.166$, $Q = 0.25$, $V_{\text{in}} = 340\,\text{V}$.

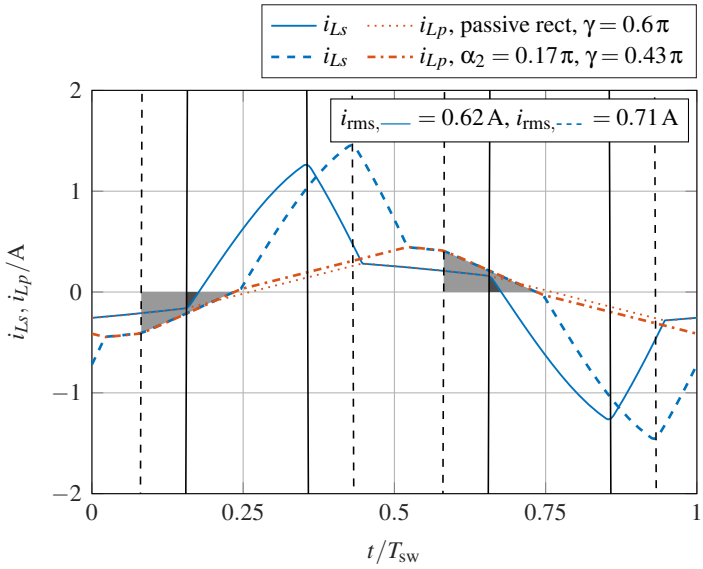

Fig. 10: Resonant tank current waveforms with improvement of ZVS charge visualised by grey shaded area; $F = 1$, $\kappa = 0.166$, $Q = 0.25$, $V_{\text{in}} = 340\,\text{V}$.

sition in the selected operating point, the optimal α_2, with the lowest $i_{Ls,\text{rms}}$, is $0.17\,\pi$ (■). Fig. 10 shows this optimal operating point as well as the waveforms of the corresponding passive rectification operating point. The instances where the input bridges change state are indicated by solid black lines for the passive rectification case, and with dashed black lines for the active rectification case. We clearly see the larger charge present for the active output case (light ▬ versus dark shaded area ▬). Furthermore, there is a change of the rms value of i_{Ls}, that is comparatively small, as the larger primary-side phase-shift for the passive rectification scheme increases the rms value of the current as well. For the passive rectification scheme $i_{Ls,\text{rms}}$ is 0.62 A, for the active output scheme 0.71 A. Even though the rms value and the losses tied to this metric increase, achieving ZVS (and with that avoiding switching losses altogether) has an overall benefit with regard to the total losses and thus the efficiency. Therefore, the active output modulation scheme can improve the ZVS behaviour at the series resonance frequency without a drastic change of rms losses.

The same reasoning holds true if the LLC is operated above its series resonance frequency. In this case, there are three different means of achieving the desired output voltage: the switching frequency, the primary-side phase-shift, and the active output modulation.

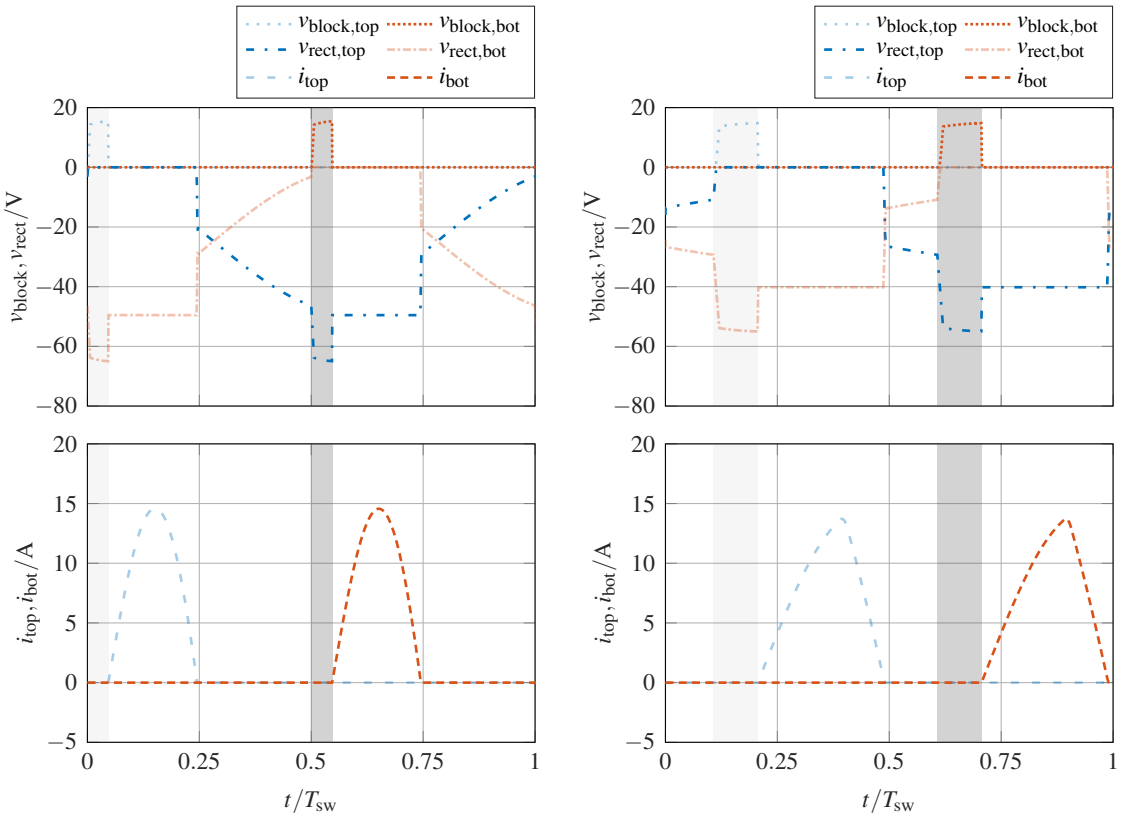

(a) $\alpha_2 = 0.08\,\pi$, $F = 0.465$, $V_{\text{out}} = 25\,\text{V}$.

(b) $\alpha_2 = 0.17\,\pi$, $\gamma = 0.43\,\pi$, $F = 1$, $V_{\text{out}} = 20\,\text{V}$.

Fig. 11: Voltages and currents of output switches for active rectification and two distinct operating points.

Secondary-side switch requirements

One aspect, that should be elaborated on, are the requirements for the secondary-side *blocking* as well as the *rectifying* switches. For this, Fig. 11 depicts the voltages and currents of the secondary-side switches for two operating points. In the top plots of Fig. 11, the voltages across the blocking *and* the rectifying switches, v_{block} and v_{rect}, are presented. In the bottom plots of the same figure, the currents through the switches, i_{top} and i_{bot} are shown[1]. To compare the passive and active rectification *intra* operating point—in contrast to *inter* operating points—the drawings in Fig. 12 are provided. As before, the time spans during which one of the output switches is actively blocking are shaded in grey. Additionally, some curves are drawn slightly transparent to improve the overall legibility.

The first operating point—$\alpha_2 = 0.08\,\pi$, $F = 0.465$—is chosen to be representative for switching frequencies below the *load independent point* and is shown in Fig. 11a and Fig. 12. This is the same operating point that was utilised for Fig. 8b. The second operating point—$\alpha_2 = 0.17\,\pi$, $\gamma = 0.43\,\pi$, $F = 1$—is chosen to be representative for operation with a significant primary-side phase-shift and is shown in Fig. 11b. Here, the same operating point was used as in Fig. 10.

In both operating points, the output currents exhibit a similar rms value if compared to their corresponding *passive* rectification case. For example, for the operating point in Fig. 11a, the rms value of the output currents, i.e. $i_{\text{top}} + i_{\text{bot}}$, is 6.59 A and 6.53 A, for the *passive* and the *active* rectification case, respectively. In Fig. 12a these currents are explicitly compared between the operating schemes. The same metric for the operating point shown in Fig. 11b also exhibits no strong dependency if comparing to the *passive* rectification case and, furthermore, is similar to the values of the first operating point. Accordingly, an increase in rms losses can be expected to mainly scale with the on-resistance of the additional blocking switch.

[1] The definitions of the voltages and the currents can be found in Fig. 5.

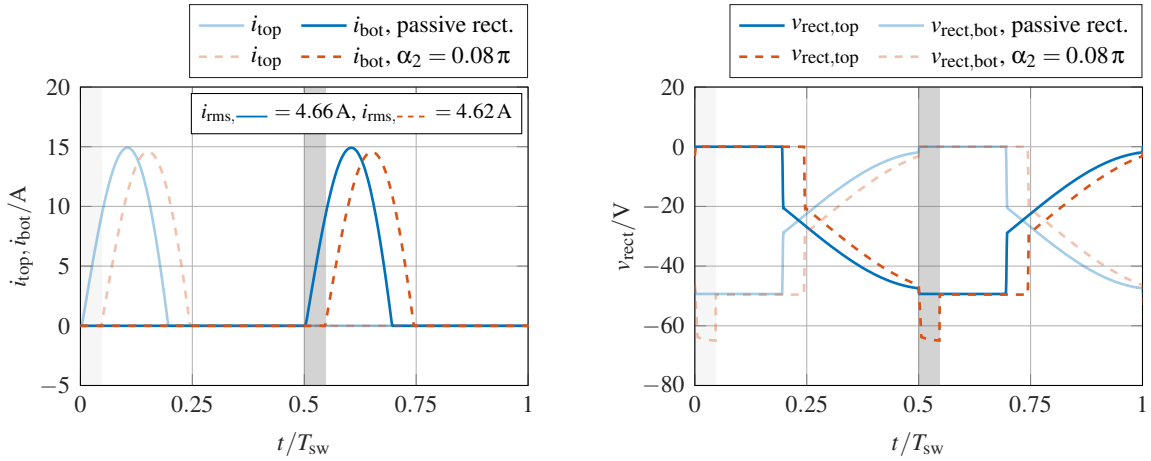

(a) Current through output switches.

(b) Voltage across *rectifying* switches.

Fig. 12: Output switch voltage and current waveforms for passive and active rectification; $F = 0.445$ (——, passive rectification), $F = 0.465$ with $\alpha_2 = 0.08\,\pi$ (- - -, active rectification), $V_{out} = 25\,V$.

On the other hand, the off-state voltages of the switches show a significantly different characteristic if the *active* rectification is used. In the respective grey-shaded areas in Fig. 11, the voltages across the *blocking* switches are about 15 V. The same voltage is visible in v_{rect} as an *additional* component on top of the corresponding *passive* rectification waveform, which is, in the ideal case, limited to $2V_{out}$. This *additional* voltage is—in general—dependent on the input voltage, V_{in}, and transfer ratio of the transformer, n. To make the differences more apparent, Fig. 12b is provided, in which the *rectifying* switch voltage of the passive rectification is juxtaposed with the voltage of the active rectification. Consequently, the *rectifying* switches have to withstand an approximately 30 % higher voltage in the chosen operating points. Here, a trade-off becomes apparent between the primary-side ZVS and circulating currents, on one hand, and the blocking capabilities of the output switches, on the other hand.

Conclusion

In this paper, the modification of adding an active output to the load-resonant LLC converter was proposed. Based on simulation results, the converter's behaviour was presented in the time and frequency domain. The main advantages of the active output LLC are the increased boost as well as the ZVS capabilities for low switching frequencies, which will enable higher efficiencies compared to a standard LLC converter. For higher switching frequencies, a combination of frequency and phase-shift modulation was presented, which also improves the ZVS behaviour.

These advantages do not come at the expense of the key benefits of the LLC converter, namely the low component count and high efficiency, which is mainly accountable to ZVS operation, as the presented topology inherits these from the state-of-the-art LLC topology. One drawback of the proposed topology is the increased control and drive effort on the secondary side. Additionally, it has to be ensured that the blocking switches do not switch off the *inductive* output current, which could result in the destruction of the respective switch. Furthermore, it is apparent that without *true* reverse blocking switches, at least one *additional* switch has to be placed in the output path, resulting in an increase in conduction losses.

We showed that the active output LLC, paired with a suitable modulation strategy, offers an additional control input that allows supplementary boosting or stepping-down of the output voltage, if required in the operating point. This increases the design space of the LLC and its transformer. The combination of both modulation strategies decouples the resonant tank's and transformer's design parameters, Q and κ—at least partially—from the achievable voltage transfer range, and thus enables optimal designs with higher efficiency.

To prove the validity of the presented topology, a prototype sub-100 W converter has been built. The results will be presented in a follow-up publication.

References

[1] H. Wu, T. Mu, X. Gao, and Y. Xing, "A secondary-side phase-shift-controlled LLC resonant converter with reduced conduction loss at normal operation for hold-up time compensation application," *IEEE Trans. Power Electron.*, vol. 30, no. 10, pp. 5352–5357, 2015.

[2] H. Wang and Z. Li, "A PWM LLC type resonant converter adapted to wide output range in PEV charging applications," *IEEE Trans. Power Electron.*, vol. 33, no. 5, pp. 3791–3801, 2018.

[3] H. Wu, Y. Lu, T. Mu, and Y. Xing, "A family of soft-switching dc–dc converters based on a phase-shift-controlled active boost rectifier," *IEEE Trans. Power Electron.*, vol. 30, no. 2, pp. 657–667, 2015.

[4] R. Steigerwald, "A comparison of half-bridge resonant converter topologies," *IEEE Trans. Power Electron.*, vol. 3, no. 2, pp. 174–182, 1988.

[5] M. P. Foster, C. R. Gould, A. J. Gilbert, D. A. Stone, and C. M. Bingham, "Analysis of CLL voltage-output resonant converters using describing functions," *IEEE Trans. Power Electron.*, vol. 23, no. 4, pp. 1772–1781, 2008.

[6] T. Duerbaum, "First harmonic approximation including design constraints," in *Intern. Telecom. Energy Conf.*, San Francisco, CA, Oct. 1998, pp. 321–328.

[7] W. Liu, B. Wang, W. Yao, Z. Lu, and X. Xu, "Steady-state analysis of the phase shift modulated LLC resonant converter," in *Proc. IEEE Energy Convers. Congr. Expo.*, Milwaukee, WI, Sep. 2016, pp. 1–5.

[8] N. Kollipara, M. K. Kazimierczuk, A. Reatti, and F. Corti, "Phase control and power optimization of LLC converter," in *Intern. Symp. Circuits and Systems*, Sapporo, Japan, May 2019, pp. 1–5.

[9] R. W. Erickson and D. Maksimović, *Fundamentals of Power Electronics*, 2nd. Norwell, MA: Kluwer Academic, 2001.